Design and Fabrication of a Bio-inspired Acceleration Sensor Using Liquid Mass Blocks

BIAN Yixiang, ZHANG Yi, ZHANG Yanjun, GONG Junjie, JIN Hong, DAI Longchao*

College of Mechanical Engineering, Yangzhou University, Yangzhou 225127, P.R.China

(Received 20 April 2017; revised 14 November 2017; accepted 9 January 2019)

Abstract: A linear acceleration sensor, which is inspired by the human balance organ, is designed and prepared. It uses a liquid mass-block and a symmetrical-electrodes metal-core polyvinylidene fluoride fiber (SMPF) as the sensor element. The output signal of the sensor has an exponential relationship with the excitation amplitude of the impacting vibration. It is capable of detecting the amplitude and the correct frequency for sinusoidal excitations using an exponential correlation. The experiments indicate that both the output signal of the sensor and the resonance frequency increase substantially with increasing diameter of the metal core. The first-order resonance frequencies of the sensors with 40, 60, and 80 μm diameter metal wires are below 10 Hz, which is near the range of human body motion frequencies.

Key words: acceleration sensor; PVDF fiber; biomimetic; liquid mass

CLC number: TM282 **Document code**: A **Article ID**: 1005-1120(2019)01-0154-08

0 Introduction

The utricular and saccular otolith organs are key elements of the human vestibular system, which is important in maintaining balance[1]. It is capable of sensing both head orientation and linear acceleration[1]. Cilia are tiny hair-like structures of sensory cells that extend from a base membrane. The hair cells of the otolithic organ are covered with a gelatine-like layer studded with tiny calcium stones called otoconia. When the head performs a rectilinear motion, the otolithic organ conducts a linear acceleration movement. Since the density of the otoconia is higher than the gelatinous membrane, the inertia force is bigger; therefore, its displacement will be smaller than for the gelatinous membrane[2]. A deformation of the sensory hair causes the sensory cell nerves to produce neural signals, which are transmitted to the vestibular center and brain through the ascending nervous system. This process converts the mechanical signals of the otolithic organ into neural signals[3].

For some existing wearable electronic devices and applications to produce a virtual reality(VR) experience, it is very important to detect the movement of the human body. The main frequencies of human body movements are below 10 Hz[4]. Existing solid-state accelerometers, such as accelerometers using cantilevers, capacity, piezo-resistivity, piezoelectricity, and electron tunneling, have higher natural resonance frequencies (>1 kHz) that are not suitable for low-frequency human-motion detection[5]. For this reason, some researchers suggest to consider bionic linear acceleration, and imitate the human capsule organ structure. This involves the use of artificial hair-sensors and a liquid mass block in the bladder organs of the lymph. Such liquid-state accelerometers are made of simple structures and utilize a low resonance-frequency of about 10 Hz, which is near the movement frequency of the human

*Corresponding author, E-mail: gjunj@126.com.

How to cite this article: BIAN Yixiang, ZHANG Yi, ZHANG Yanjun, et al. Design and Fabrication of a Bio-inspired Acceleration Sensor Using Liquid Mass Blocks[J]. Transactions of Nanjing University of Aeronautics and Astronautics, 2019, 36(1): 154-161.

http://dx.doi.org/10.16356/j.1005-1120.2019.01.015

body[5].

In such a bionic acceleration sensor, the design of the bionic hair-sensing element is most important. Many researchers have developed a variety of artificial hair sensing elements to detect the acceleration of surrounding water-flow[6]. The basic structure is a sensor element in combination with a cantilever structure. The cantilever beam is immersed in water or around the cover. When the water moves the cantilever beam, the cantilever beam deforms / bends. The acceleration of the cantilever is measured by measuring the deformation of the cantilever beam. There are four types of artificial-hair sensors: (1) In piezoresistive hair-sensors[7], a piezoresistive element is located in the root plane of the vertical hair. When the hair is bent, the resistance of the piezoresistive element changes. By measuring the change in resistance, it becomes possible to calculate the bending deformation of the hair, and derive the acceleration of the water[7-8]. (2) In capacitive hair-sensors, the cantilever structure includes a micro-movable capacitor at the root of the hair. When the cantilever beam bends, the distance between the two moving capacitive plates changes. The deformation of the cantilever beam is calculated by measuring this change in capacitance[9]. (3) In the piezoelectric hair-sensor, a micro-piezoelectric ceramic film is used which consists of sensing elements that are arranged in accordance with the array around the hull[10-11]. By measuring the change of the surface charge in each sensor element, the acceleration of water can be measured at each point directly[12]. (4) In artificial muscle hair-sensors, the ion-exchange polymer metal composite (IPMC) is made of fiber and immersed in the water[13]. The IPMC has a three-tier structure. When the water accelerates the fiber, electrical signals are generated that permit the calculation of the acceleration.

In this paper, we use a bimodal hair-sensor SMPF (symmetrical-electrode metal-core PVDF fiber), which can perceive its own bending deformation as the sensing element and use a liquid mass to detect linear acceleration-similar to the human balance sensor. The resonance frequency of this linear-acceleration sensor is about 10 Hz, which is suitable for the detection of both human and robotic body movements.

1 Design and Fabrication of Sensor

The sensor described in this paper imitates the human otolithic organ using a SMPF instead of the sensory hair. It also uses a liquid, which replaces the mass block of the otoconia, to sense linear acceleration. The specific structure of the sensor is shown in Fig. 1(a). A closed circular section pipe is filled with liquid. The inner diameter of the long pipe is 1.5 mm, the expansion part 2.5 mm, and the spherical part 4 mm. The SMPF cantilever beam is attached to the inner wall of the expansion part of the pipe, which is suspended in the liquid to serve as the sensing element. In order to improve the sensitivity of the sensor, we wrapped a layer of silicone rubber around the SMPF to imitate the structure of the otolith.

The structure of the SMPF is shown in Fig. 1 (b)[14]. One stainless-steel wire, with a diameter between 40—100 μm in the center of the fiber, is wrapped with a 10 μm PVDF layer with two symmetrical surface-electrodes. A 40 μm thick and 2 mm long silicone layer covers the surface of the SMPF. During the polarization process of the SMPF, the central stainless-steel wire functions as the first electrode and the two connected surface electrodes as second electrode. After polarization, the PVDF sector covered with electrodes has become polarized and piezoelectric. The direction of polarization is diametric. The PVDF portion of the surface is not covered by the electrode, and is neither polarized nor piezoelectric[13]. When the SMPF of the cantilever beam structure causes a deformation in the sensor, electric charges appear on the surface electrodes due to the piezoelectric effect. Because the two surface electrodes are completely symmetrical, the electric charge on the electrodes is the same but with opposite polarities. The two surface electrodes are connected to the two signal-inputs of a sensing circuit. The degree of bending (deformation) of the SMPF can then be calculated consider-

ing the charge at the electrode[16]. The pressure of the liquid of the cantilever beam can be obtained considering the structure of the cantilever beam, and the linear vibration of the sensor is obtained.

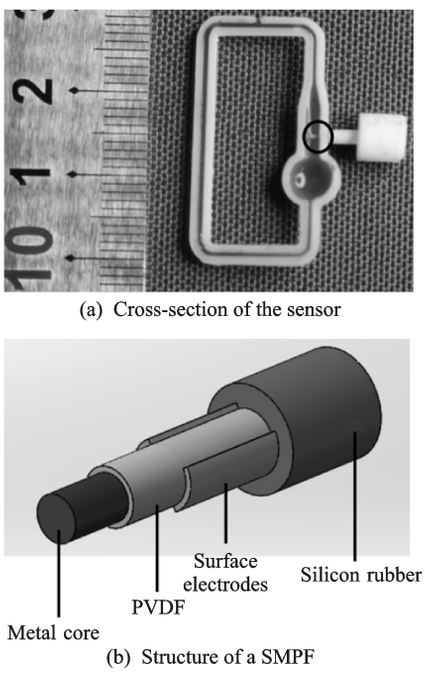

Fig.1 Structure of the sensor

2 Modelling of Sensor

As can be seen in Fig.1(a), when the pipe of the sensor undergoes a linear impact or vibration, the displacement $u(t)$ can be written as

$$u(t)=U_0(1-e^{-\tau t}) \tag{1}$$

where U_0 is the initial amplitude of the vibration, and τ is the time constant. The smaller τ is, the more distinct the characteristics of impact and vibration are. By then, the SMPF cantilever beam moves synchronously with the pipe. However, due to differences in inertia, the movements of the liquid and the pipe cannot be synchronous, and a relative movement between the liquid and the SMPF cantilever beam emerges. The flow velocity of the liquid can be obtained as $v=\dot{u}(t)$. As a result, the SMPF cantilever can generate bending deformation because of the equispaced liquid load. Since the angle of deflection of the cantilever is small, the deformation of the SMPF can be assumed pure bending-deformation. Based on Eq.(1), the equispaced load F received by the SMPF is

$$F=\frac{1}{2}\rho_L v^2(RL)C_d \tag{2}$$

where ρ_L is the density of the liquid, ν the flow velocity, R the diameter of the cantilever, L the length of the cantilever, and C_d the local coefficient of drag and determined by the local Reynolds number. Under the action of the equispaced load F, the bending moment produced by the SMPF is[1]

$$M=\frac{1}{2}F(L-z)^2 \tag{3}$$

Using the piezoelectric equations, one can obtain the electric charge on the electrode of the SMPF[7].

$$Q=\int_0^L\int_{\frac{\pi-\alpha}{2}}^{\frac{\pi+\alpha}{2}} d_{31}\frac{MR_c\sin\theta}{s_{11}^E EI}R_c\,d\theta dz \tag{4}$$

where d_{31} is the piezoelectric constant, I the moment of inertia, and E the elastic modulus. According to Eq.(4), when the pipe undergoes impact vibration excitation, assuming that time is constant, the output Q and the impact amplitude U_0 are exponentially related. After calibration, the amplitude of the impact vibration can be calculated from the detection signal of the sensor. When the pipe receives sinusoidal excitation, the displacement $u(t)$ is

$$u(t)=U_0\sin(\omega t) \tag{5}$$

where ω is the frequency of the vibration. Inserting Eq.(5) into Eqs. (2)—(4), we obtain the electric charges at the output, which are exponentially related with the amplitude U_0. The angle of deflection of the SMPF cantilever beam can be represented as[17]

$$\theta=\sqrt{C_1^2+C_2^2}\sin(\omega t+\varphi) \tag{6}$$

where C_1 and C_2 are constant coefficients as defined in Ref.[9]. These increase linearly with the amplitude of the vibration U_0. The phase φ is determined by C_1 and C_2.

When the dimensions of the SMPF are known, the sensed electric charge Q can be obtained using Eq.(6). When the pipe receives sinusoidal excitation, the output signal of the sensor is sinusoidal as well, and its frequency is the same as for the excitation. The amplitude follows an exponential relationship with the square of the amplitude of the vibration. Thus, the excitation frequency can be obtained from the sensor frequency, and the vibra-

tion amplitude can be obtained from the amplitude of the electric charge.

3 Results and Discussion

In order to verify the ability of the sensor to detect linear acceleration, we built the following setup: The sensor was attached to the excitation head of a vibration exciter. The sensed electric charges of the SMPF pass through a charge amplifier and a data acquisition card of a computer.

Fig.2(a) shows the sensed signals and the displacement when the sensor detects the shock excitation of the vibration exciter. During the response process, an abrupt up-ward displacement occurs at the pipe. At this moment, the SMPF and the pipe of the sensor move upward simultaneously. Due to inertia, the liquid in the pipe attempts to stay at its original place to produce a relative downward motion to the SMPF, which produces a downward equispaced load for the SMPF cantilever beam. The cantilever beam also carries a downward acting equispaced load due to its inertia. Under the combined action of two downward acting equispaced loads, the cantilever beam bends downward. Because of the deformation due to bending and the piezoelectric effect, the wrapped SMPF in the cantilever beam produces negative charges. As the pipe continues to rise, the speed of the internal liquid decreases gradually and eventually reaches zero relatively to the motion speed of the pipe wall. This is the result of the tension between the bottom of the pipe and the adhesive force of the pipe wall. During this process, the equispaced load acting on the cantilever beam, which is caused by the internal liquid, also decreases gradually to reach zero. This leads to the maximum bending deformation of the cantilever beam and the maximum SMPF output charge. Subsequently, because of its own flexibility, the cantilever beam returns gradually to reach its equilibrium position. The SMPF output-charges also increase from the maximum negative value to zero.

When the pipe reaches its highest point under the action of the vibration exciter, it moves downward rapidly. This produces the same motion as the cantilever beam. Due to inertia, the liquid will attempt to keep the upward motion and develop a relative motion in the opposite direction. This creates an upward equispaced load force for the cantilever beam, and due to inertia, the cantilever beam itself produces an equispaced load force upward. Under the action of the two upward pointing equispaced load forces, the cantilever beam produces an upward bending deformation and the SMPF outputs charges with positive polarity. Because of the pipe tension and adhesive force, the equispaced load acting on the cantilever beam by the liquid inside the pipe, gradually decreases and reaches zero. The cantilever beam also reaches the maximum upward-bending deformation. By then, the positive electric-charge output of the SMPF reaches a maximum, which is slightly delayed with respect to the maximum displacement of the pipe. Then, the pipe returns to the equilibrium position and the SMPF generated response charge gradually returns to zero. During the whole recovery process, the behavior of the SMPF generated output charge is almost the same as that of the pipe displacement. However, there is a lag in time.

The SMPF responses for the same time constant and impact excitation with different amplitudes are shown in Fig.2(b). For impact excitation with different amplitudes, the curves of the SMPF output electric charges are almost the same, but the maximum charge increases. The impact vibration diagram shown in Fig.2(c) is obtained by taking the displacement amplitude of the pipe in each impact process as the abscissa and the SMPF response charge amplitude as the ordinate. Fig.2(c) shows that there is an exponential relationship between the maximum response amplitude of the SMPF and the maximum displacement amplitude of the pipe. This is consistent with the relationship between charge Q and amplitude U_0 in Eq.(4), which suggests that the impact vibration amplitude of the pipe can be sensed using the maximum output charge of the SMPF in impact vibration. Furthermore, with an increasing metal-wire diameter, the area of the PVDF layer in the SMPF also increases, as well as the SMPF output charge signal and the sensitivity of

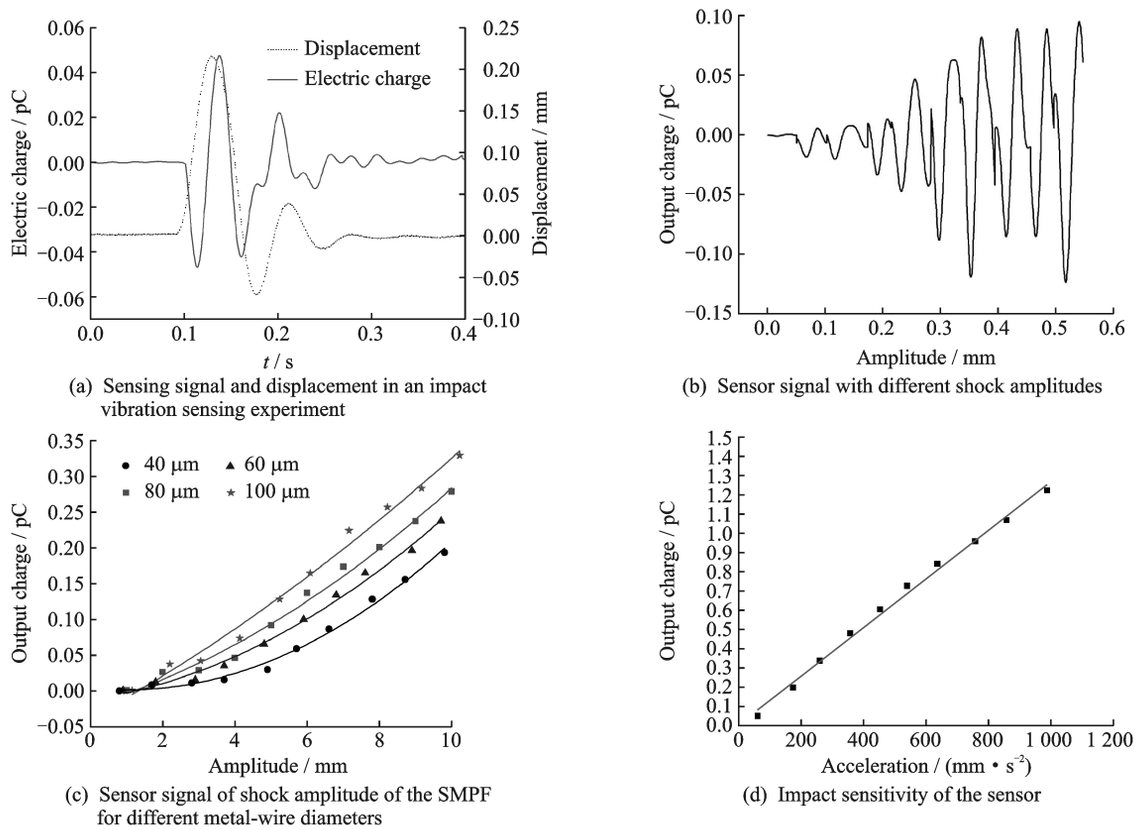

(a) Sensing signal and displacement in an impact vibration sensing experiment

(b) Sensor signal with different shock amplitudes

(c) Sensor signal of shock amplitude of the SMPF for different metal-wire diameters

(d) Impact sensitivity of the sensor

Fig.2 Shock vibration sensing experiment

the sensor will gradually increase.

When the vibration exciter produces sinusoidal excitations for the sensor, the SMPF also outputs sinusoidal signals with a frequency identical to the one of the vibration exciter (Fig.3(a)). This verifies that the sensor can detect the excitation frequency of the vibration exciter. However, there is a certain phase difference between the vibration mode of the sensor and that of the vibration exciter, which relates to the excitation frequency. The relationship between this phase difference and the excitation frequency is shown in Fig.3(b). The phase difference decreases gradually with increasing excitation frequency. For a 5 Hz excitation, the amplitude of the SMPF output sinusoidal signal also increases with increasing amplitude of the pipe vibration displacement (Fig.3(c)). We set the amplitude of the pipe vibration as the abscissa, and the amplitude of the SMPF response charge as the ordinate. The specific relationship between the vibration amplitude and the response signal amplitude is shown in Fig.3(d). It indicates that there is a square relation between the SMPF signal amplitude and the received excitation. The relation between the SMPF sensing signals and the excitations received by the pipe also confirms the theoretical prediction expressed in Eq.(6). This prediction includes that when the pipe receives sinusoidal excitations, the SMPF also outputs sinusoidal signals of the same frequency as the excitations. Furthermore, the higher the frequency is, the smaller the phase difference is. The amplitude of the SMPF output sinusoidal signals follows a square relationship with the excitation amplitude.

The frequency response of the sensor is shown in Fig.3(e). In this figure, the vibration exciter produces sinusoidal excitations for the pipe and changes the excitation frequency, while maintaining constant amplitude. Although the SMPF is still outputting sinusoidal signals, its amplitude changes with the changes of frequency. As indicated in the figure, with increasing metal-wire diameter, the resonance frequency of the sensor increases to 1.8, 3.8, 6.6, and 10.4 Hz. In the phase of resonance frequency, the amplitude of the output signal also increases gradually. The first-order resonance frequencies for the 40, 60 and 80 μm metal wire sensors are all be-

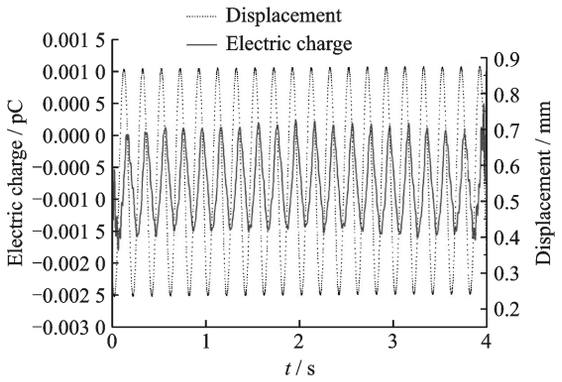

(a) Sensing signal and displacement at 5 Hz sinusoidal vibration

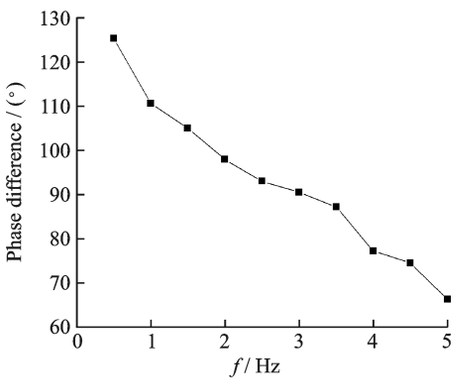

(b) Phase difference between sensing signal and displacement in different frequency vibrations

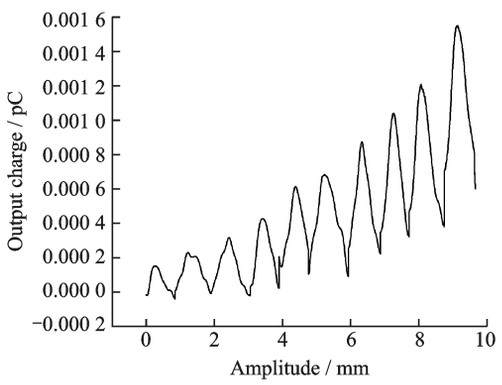

(c) Sensing signals with different amplitudes and 5 Hz sinusoidal vibration

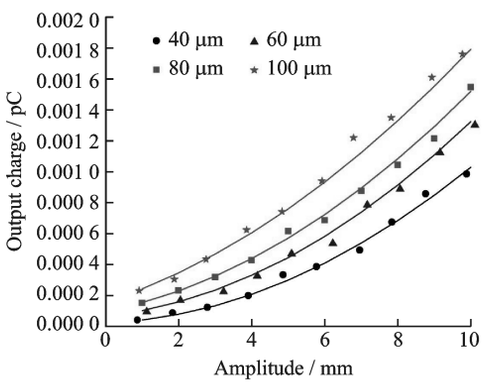

(d) Sensing signal of 5 Hz sinusoidal vibration amplitude of SMPF with different metal-wire diameters

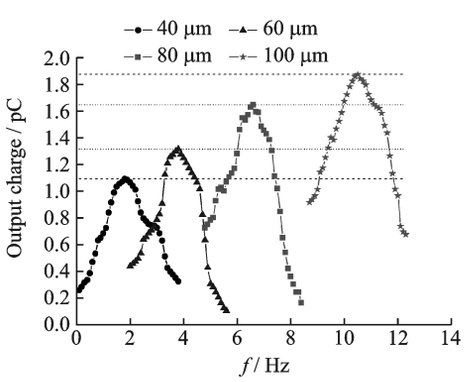

(e) Resonance frequency of SMPF with different diameters of metal wires

Fig.3 Sinusoidal vibration sensing experiment

low 10 Hz, i.e., within the frequency range of the human body. Depending on the specific application, it is desirable to select metal wires with different diameters to obtain different first-order resonance frequencies.

Based on the calibration specification for shock accelerometers (JJF 1153—2006), The impact sensitivity of a linear-acceleration sensor is calculated using

$$S_{sh} = \frac{U_p}{a_p} \tag{7}$$

where S_{sh} is the impact sensitivity, U_p the charge peak, and a_p the acceleration peak.

In the sensor test of the fiber with a metal-core diameter of 40 μm, the impact sensitivity was calculated using Eq.(7), and the experimental results are shown in Fig.3(d). The figure reveals that the output signal of the sensor and the acceleration signal are related linearly.

To measure the linear acceleration of the substrate, the sensor is mounted on the substrate. When the substrate is subjected to acceleration, the output signals of the sensor are used in Eq.(7), and the acceleration of the matrix can be calculated.

4 Conclusions

An acceleration sensor similar to the one used in the vestibular system of the human body was designed using an SMPF, which imitates human sensory hair cells, and a liquid, which imitates the otoconia and the colloid mass block. The sensor detects both linear shock and vibration. Thanks to the proposed governing equations, the sensor can detect the amplitude of impacting vibration. The sensor is also capable of detecting the frequency and amplitude of sinusoidal excitations. Experimental results show that the resonance frequency of the sensor is below 10 Hz, which is close to the range of human body motion. The biomimetic linear acceleration sensor described in this paper can not only be used to detect the motion of a human head, but also be used to detect movements of other body parts to enable life-like simulations, or as a key component of a balancing system in robots. The sensor can also be used in portable electronic devices, especially virtual-reality devices to detect the linear acceleration of human body parts.

References

[1] BOSELLI F, OBRIST D, KLEISER L. Vortical flow in the utricle and the ampulla: A computational study on the fluid dynamics of the vestibular system[J]. Biomech Model Mechanobiol, 2013, 12(2): 335-348.

[2] MARIANELLI P, BERTHOZ A, BENNEQUIN D, et al. Crista egregia A geometrical model of the crista ampullaris, a sensory surface that detects head rotations[J]. Biological Cybernetics, 2015, 109(1): 5-32.

[3] DAVIDOVICS N S, FRIDMAN G Y, CHIANG B, et al. Effects of biphasic current pulse frequency, amplitude, duration, and interphase gap on eye movement responses to prosthetic electrical stimulation of the vestibular nerve[J]. IEEE Transactions on Neural Systems & Rehabilitation Engineering, 2011, 19(1): 84-94.

[4] ANDREOU C M, PAHITAS Y, GEORGIOU J. Bio-inspired micro-fluidic angular-rate sensor for vestibular prostheses[J]. Sensors, 2014, 14(7): 13173-13185.

[5] ZENG H, ZHAO Y. Dynamic behavior of a liquid marble based accelerometer[J]. Applied Physics Letters, 2010, 96(11): 114104.

[6] TAN Shizhe. Underwater artificial lateral line flow sensors [J]. Microsystem Technologies, 2014, 20 (12): 2123-2136.

[7] QUALTIERI A, RIZZI F, TODARO M T, et al. Stress-driven AlN cantilever-based flow sensor for fish lateral line system [J]. Microelectronic Engineering, 2011, 88(8): 2376-2378.

[8] YANG Y C, KLEIN A, BLECKMANN H, et al. Artificial lateral line canal for hydrodynamic detection[J]. Applied Physics Letters, 2011, 99(2): 481-499.

[9] IZADI N, de BOER M J, BERENSCHOT J W, et al. Fabrication of superficial neuromast inspired capacitive flow sensors[J]. Journal of Micromechanics & Microengineering, 2010, 20(8): 085041.

[10] CHEN W H, WANG Y X, SHEN X, et al. Neural network PID real-time control for active vibration reduction using piezoceramics stacks[J]. Journal of Nanjing University of Aeronautics & Astronautics, 2014, 46 (4) :587-593. (in Chinese)

[11] LIU X R, HUANG W Q, SUN M X. A novel 2D piezo-nanopositioning stage based on triangle amplifier mechanism[J]. Transactions of Nanjing University of Aeronautics & Astronautics, 2017, 34(1):1-8.

[12] ASADNI M, KOTTAPALLI A G K, SHEN Z Y, et al. Flexible and surface-mountable piezoelectric sensor arrays for underwater sensing in marine vehicles [J]. IEEE Sensors Journal, 2013, 13(10): 3918-3925.

[13] JING X M, MIAO J M, XU T, et al. Vibration characteristics of micromachined piezoelectric diaphragms with a standing beam subjected to airflow[J]. Sensors & Actuators A Physical, 2010, 164(1/2): 22-27.

[14] BIAN Y X, LIU R R, HUANG X M, et al. Design and fabrication of a metal core PVDF fiber for an air flow sensor [J]. Smart Materials and Structures, 2015, 24(10): 105001.

[15] BIAN Y X, LIU R R, SHEN H. Fabrication of a polyvinylidene difluoride fiber with a metal core and its application as directional air flow sensor[J]. Functional Materials Letters, 2015: 1650001.

[16] BIAN Y X, LIU R R. Fabrication of a biomimetic piezoelectric polyvinylidene difluoride (PVDF) fibre with a metal core and its application in vibration sensors[J]. Transactions of the Institute of Measurement and Control, 2016: 0142331216649020.

[17] CHEN N C, TUCKER C, ENGEL J M, et al. Design and characterization of artificial haircell sensor for flow sensing with ultrahigh velocity and angular sensitivity[J]. Journal of Microelectromechanical Systems, 2007, 16(5): 999-1014.

Acknowledgements This work was supported by the National Natural Science Foundation of China (Nos. 51775483

and 51275447); the Research Innovation Program for College Graduates of Jiangsu Province (No.SJLX_0589).

Authors Prof. **BIAN Yixiang** received his Ph.D. degree from Nanjing University of Aeronautics and Astronautics, Nanjing, China, in 2009. Now he is an associate professor of School of Mechanical Engineering Yangzhou University, and his research focuses on the biomimetic sensor and the biological perception mechanism. Mr. **ZHANG Yi** is a graduate student of School of Mechanical Engineering of Yangzhou University. His research focuses on the bionic sensor.

Mr. **ZHANG Yanjun** is a graduate student of School of Mechanical Engineering of Yangzhou University. His research focuses on the smart sensor.

Prof. **GONG Junjie** received his Ph.D. degree from Nanjing University of Aeronautics and Astronautics, Nanjing, China, in 2007. Now he is a professor and the dean of School of Mechanical Engineering Yangzhou University. His research focuses on the mechanical design and theory and the engineering mechanics.

Prof. **JIN Hong** received his Ph.D. degree from Southeast University, Nanjing, China, in 2016. Now he is an associate professor of School of Hydraulic Energy and Power Engineering of Yangzhou University.

Prof. **DAI Longchao** received his Ph.D. degree from Nanjing University of Aeronautics and Astronautics, Nanjing, China, in 2008. Now he is an associate professor of School of Mechanical Engineering of Yangzhou University. His research focuses on the flexible electronic device, smart material structure, and destructive mechanics.

Author contributions Prof. **GONG Junjie** designed the study. Prof. **BIAN Yixiang** complied the models, conducted the analysis, interpreted the results and wrote the manuscript. Mr. **ZHANG Yi** contributed data and model components. Mr. **ZHANG Yanjun** contributed data and model components. Dr. **JIN Hong** contributed data for the analysis of the model. Dr. **DAI Longchao** contributed to the discussion and background of the study. All authors commented on the manuscript draft and approved the submission.

Competing interests The authors declare no competing interests.

(Production Editor: Zhang Huangqun)